Available online at www.sciencedirect.com

SciVerse ScienceDirect

Ceramics International 38 (2012) 4715–4722

CERAMICS INTERNATIONAL

www.elsevier.com/locate/ceramint

Relationship between elastic and mechanical properties of dental ceramics and their index of brittleness

Humberto Naoyuki Yoshimura [a,*], Carla Castiglia Gonzaga [b,c], Paulo Francisco Cesar [b], Walter Gomes Miranda Jr. [b]

[a] Center for Engineering, Modeling and Applied Social Science, Federal University of ABC, Santo André, Brazil
[b] Department of Biomaterials and Oral Biochemistry, School of Dentistry, University of São Paulo, São Paulo, Brazil
[c] Masters Program in Clinical Dentistry, Positivo University, Curitiba, Brazil

Received 6 December 2011; received in revised form 11 February 2012; accepted 19 February 2012
Available online 25 February 2012

Abstract

The purpose of the study was to verify the effects of a number of materials' parameters (crystalline content; Young's modulus, E; biaxial flexure strength, σ_i; Vickers hardness, VH; fracture toughness, K_{Ic}; fracture surface energy, γ_f; and index of brittleness, B) on the brittleness of dental ceramics. Five commercial dental ceramics with different contents of glass phase and crystalline particles were studied: a vitreous porcelain (VM7/V), a porcelain with 16 vol% leucite particles (d.Sign/D), a glass-ceramic with 29 vol% leucite particles (Empress/E1), a glass-ceramic with 58 vol% lithium-disilicate needle-like particles (Empress 2/E2), and a glass-infiltrated alumina composite with 65 vol% crystals (In-Ceram Alumina/IC). Discs were constructed according to manufacturers' instructions, ground and polished to final dimensions (12 mm × 1.1 mm). Elastic constants were determined by ultrasonic pulse-echo method. σ_i was determined by piston-on-3-balls method in inert condition. VH was determined using 19.6 N load and K_{Ic} was determined by indentation strength method. γ_f was calculated from the Griffith–Irwin relation and B by the ratio of HV to K_{Ic}. IC and E2 showed higher values of σ_i, E, K_{Ic} and γ_f, and lower values of B compared to leucite-based glass-ceramic and porcelains. Positive correlations were observed for σ_i versus K_{Ic}, and K_{Ic} versus $E^{1/2}$, however, E did not show relationship with HV and B. The increase of crystalline phase content is beneficial to decrease the brittleness of dental ceramics by means of both an increase in fracture surface energy and a lowering in index of brittleness.

Keywords: C. Mechanical properties; C. Fracture; C. Toughness; E. Biomedical applications; Ceramics

1. Introduction

The development of new all-ceramic restorative materials has been triggered by the search for esthetics, biocompatibility and strength. Despite the great clinical success of metal-ceramic crowns and fixed partial dentures, the increasing strength of core-veneered all-ceramic materials has also made possible the construction of metal-free restorations with more reliability. Now several all-ceramic systems are available for the construction of all-ceramic restorations. Among these, the most popular examples are leucite-reinforced porcelains, glass-ceramics, glass-infiltrated ceramic composites, and polycrystalline ceramics [1–8]. However, it is well recognized that the main drawback of all-ceramic restorations is their inherent brittleness and inability to undergo plastic deformation, resulting in high fracture rates in clinical trials [9–12].

To understand the fracture behavior of all-ceramic restorations, fracture mechanics principles are particularly important and can shed some light onto the fracture process and its causes. Since all-ceramic components contain intrinsic and extrinsic flaws, it is important to know what flaw size can be tolerated in a structure and what the expected lifetime of a defect-containing structure will be. The first fundamental and significant work on defects acting like stress concentrators was published in 1913 by Inglis [13], who demonstrated that sharp cracks are much more deleterious than blunt ones.

In the 1920s, Griffith developed his world famous energy-balance approach, establishing a relationship between fracture

* Corresponding author at: Universidade Federal do ABC, Centro de Engenharia, Modelagem e Ciências Sociais Aplicadas, Rua Santa Adélia 166, 09210-170 Santo André, SP, Brazil. Tel.: +55 11 49963166; fax: +55 11 49963166.
E-mail address: humberto.yoshimura@ufabc.edu.br (H.N. Yoshimura).

0272-8842/$36.00
doi:10.1016/j.ceramint.2012.02.056

strength and crack size [14]. For ductile materials, Griffith's original work had to be later modified by Irwin [15]. Irwin suggested that the Griffith's equation should be rewritten to add the elastic deformation energy involved in the fracture process. Instead of developing an explicit relationship between the energy-consuming parameters, Irwin chose the parameter G (named after Griffith), which is the strain energy release rate.

While the Griffith's approach provides great understanding of the fracture process, an alternative method that studies directly the stress fields near the crack tip has gained attention in the materials science field. In fracture mechanics, the cracks can be characterized in terms of the stress intensity factor (K), which quantifies the stress field around a crack in a predominantly elastic material. In 1958, Irwin associated the concepts of Inglis and Griffith and showed that the strain energy release rate (G) is a function of the stress intensity factor (K) [16].

Rearranging the Griffith's equation, the stress intensity factor at the crack tip (K_I, I denotes uniaxial tensile or opening mode), which is also called K_{Ic} (critical stress intensity factor), is related to the stress at fracture in mode I according to the equation:

$$K_{Ic} = \sigma_f Y \sqrt{a} \quad (1)$$

where Y is a dimensionless constant that depends on the loading mode, the shape and dimensions of the material and the geometry and length of the crack, and a is the length of the crack from which the fracture propagates. K_{Ic} is a constant for a given material and is commonly referred to as fracture toughness. Eq. (1) can also be considered a failure criterion, since the brittle fracture of a material will occur when the product of the stress applied by the square root of a crack size is equal to or greater than the material's fracture toughness value.

Elastic modulus and fracture toughness are inherent properties of great importance for dental ceramics. Elastic modulus represents the stiffness of a material within the elastic range when tensile or compressive forces are applied [17] and is also an indication of the amount of reversible deformation that will occur in a structure when a load is applied to it. At the atomic scale, elastic strain can be expressed as a measure of the resistance to pulling apart adjacent atoms, expressed as small changes in inter-atomic spacing caused by stretching of bonds [18]. The fracture toughness may be defined as the measure of a material's ability to absorb energy from elastic deformation, in relation to the level of tensile stress that can be achieved near the crack tip before the initiation of catastrophic fracture [19]. Dental ceramics, as are all brittle materials, are unable to absorb appreciable quantities of elastic strain energy prior to fracture and fracture toughness can be considered a measure of the strain-energy absorbing ability of a brittle material [19].

All dental ceramics tend to fail at a critical strain of approximately 0.1% [20] and, for this reason, it has been argued that any increase in strength and toughness can only be achieved by an increase in the elastic modulus [21]. Several studies have already determined the physical and mechanical properties of commercial dental ceramics, such as elastic modulus and fracture toughness [1,2,21,22]. However, to the authors' knowledge, the relationship between these two properties has never been explored in dental materials, in spite of the fact that according to the Griffith–Irwin equation ($K_{Ic} = \sqrt{2E\gamma_s}$, in plane stress – where E is the Young's modulus, and γ_s is the surface energy per unit area), they are supposed to be positively correlated. For polycrystalline or multi-phase materials this relationship can be more complex, since elastic modulus can vary on micro-scale level at the crack front, and alternative strain-energy consumption mechanisms (deflection, crack bridging, micro-cracking, phase transformation) can be activated. To take into account the effects of toughening mechanisms, γ_s is usually replaced by γ_f, fracture surface energy (energy to create unit surface area) [23].

K_{Ic} and γ_f are considered suitable brittleness parameters when the loading is purely elastic (e.g. fracture in tension or thermal shock fracture), but when contact stresses are involved (as in scratch, impact, wear, erosion and machining events) other brittleness parameters which compare deformation to fracture processes may be more useful [24]. The ratio of hardness to toughness, H/K_c, determined under sharp contact like a Vickers indenter has been proposed as a simple brittleness parameter, B, since H is a measure of resistance to deformation and K_c is the resistance to fracture [25]. It seems this parameter has not been applied yet to evaluate dental ceramics.

Therefore, the objective of the present study was to determine the effects of a number of materials' parameters, such as crystalline content, Young's modulus (E), biaxial flexure strength (σ_i), Vickers hardness (VH), fracture toughness (K_{Ic}), fracture surface energy (γ_f;) and index of brittleness (B) on the brittleness of dental ceramics. The main hypothesis tested was that strong correlations would be found between the parameters analyzed.

2. Materials and methods

The dental ceramics used in this study are described in Table 1. Materials were selected to provide different types of clinically relevant microstructures. Fifteen disks (12 mm in diameter and 2 mm thick) of each material were produced according to each manufacturer's instructions. Porcelains were prepared by the vibration–condensation method and sintered in a dental porcelain furnace (Keramat I, Knebel, Porto Alegre, Brazil) following the firing schedules recommended by the manufacturers. Glass-ceramics were processed by the heat-press technique using a specific oven (EP 600, Ivoclar Vivadent, Schaan, Liechtenstein). In-Ceram Alumina composite was processed by a lanthanum-silicate glass infiltrating a porous partially sintered alumina preform made by slip casting. The sintering of alumina preform and the glass infiltration cycles were carried out in a special furnace (InCeramat II, Vita Zahnfabrik, Bad Sackingen, Germany). All disks were machined to reduce thickness to 1.3 mm, following the guidelines in ASTM C 1161 [26]. Then, one of the disk surfaces was mirror polished using a polishing machine (Ecomet 3, Buehler, Lake Bluff, IL, USA) with diamond

Table 1
Description of the materials used in the study.

Material	Manufacturer/Brand Name	Manufacturer's description
V	Vita Zahnfabrik/VM7	High-fusing porcelain to be used with alumina frameworks. Fusing temperature: 970 °C
D	Ivoclar Vivadent/d.Sign	Low-fusing, leucite-based porcelain, used for metal-ceramic or all ceramic restorations, containing leucite particles and crystals of fluorapatite. Fusing temperature: 875 °C
E1	Ivoclar Vivadent/IPS Empress	Heat-pressed, leucite-based glass-ceramic, used for inlays, onlays, veneers and crowns.
E2	Ivoclar Vivadent/IPS Empress 2	Heat-pressed, glass-ceramic with lithium dissilicate, used as core material in crowns and bridges.
IC	Vita Zahnfabrik/In-Ceram Alumina	Glass-infiltrated alumina composite, used as core material in crowns and bridges.

suspensions (45, 15, 6 and 1 μm). The final dimensions of the disk samples were approximately 12 mm × 1.1 mm.

The Young's modulus and Poisson's ratio of each material was determined by the pulse-echo method ($n = 10$), according to ASTM E 494-95 [27], using a device capable of emitting and receiving 200 MHz ultrasonic pulses (pulser-receiver 5900 PR, Panametrics, Waltham, MA, USA) coupled with 20 MHz longitudinal and transversal wave transducers (V208-RM and V222-RM model, Panametrics, Waltham, MA, USA). A coupling paste (Couplant SWC, Panametrics, Waltham, MA, USA) was applied between the specimen and the transducer to enhance the ultrasonic pulse signals. The time of flight of the ultrasonic pulse was measured with an oscilloscope (TDS 1002, Tektronix, USA) and the thickness of the sample was measured with a digital micrometer (Mitutoyo, São Paulo, Brazil). Sonic velocities were calculated by: $2\,t/f$, where t is the specimen thickness and f is the time of flight. The specimens' densities were determined by the Archimedean principle [28]. The Young's modulus (E) and the Poisson's ratio (υ) were calculated according the following equations:

$$E = \rho\left[\frac{(3V_t^2V_l^2 - 4V_t^4)}{(V_l^2 - V_t^2)}\right] \tag{2}$$

$$\upsilon = 0,5\left[\frac{(V_l^2 - 2V_t^2)}{(V_l^2 - V_t^2)}\right] \tag{3}$$

where ρ is the density and V_l and V_t are, respectively, the longitudinal and the transversal wave velocities.

To confirm the expected positive correlation of fracture strength and fracture toughness (Eq. (1)), ten specimens of each material were fractured in biaxial flexure using a piston-on-3-balls fixture in a universal testing machine (MTS Syntech 5G, São Paulo, Brazil) in inert condition, with a high stress rate (100 MPa/s) and with the surface subjected to tensile stress coated with a layer of silicone oil to minimize the effects of environment-assisted subcritical crack growth (SCG). The inert fracture strength (σ_i) was chosen because the differences on susceptibility for SCG among the materials tested could make this analysis difficult. Fracture stress was calculated using the equations given in the ASTM F 394-78 standard [29]. Further details about the test procedure can be found elsewhere [30].

Vickers hardness was determined by making ten indentations on the polished surfaces of fragments obtained in the biaxial flexure test. Specimens were indented in a Vickers microhardness tester (MVK-H-3, Mitutoyo, Kawasaki, Japan), using a load of 19.6 N and dwell time of 20 s. Vickers hardness (HV) was calculated according to the following equation [31]:

$$HV = \frac{1.8544P}{d^2} \tag{4}$$

where P is the load and d is the mean diagonal of the indentation.

Fracture toughness, K_{Ic}, was determined by the indentation strength (IS) method. A Vickers impression (load of 9.8 N for porcelains, 19.6 N for glass-ceramics and 49 N for IC) was introduced in the geometrical center of the polished surface of the disks and the fracture stress, σ_f, of the indented specimens was determined in a flexural strength test. Immediately after indentation, the indented region was covered with a drop of silicone oil to minimize the effects of slow crack growth. Disk specimens were fractured in a biaxial flexure test (piston-on-three-balls method), using a universal testing machine (Syntech 5G, MTS, São Paulo, Brazil) at a crosshead speed of 0.5 mm/min. Experiments were carried out in air (~22 °C, 60% RH) and five specimens were tested in each experimental condition. The value of K_{Ic} was then calculated by [32]:

$$K_{Ic} = \eta\left(\frac{E}{H}\right)^{1/8}(\sigma_f P^{1/3})^{3/4} \tag{5}$$

where η is a geometric constant, which depends on crack and indenter shapes, E is Young's modulus, P is impression load (9.8 N for porcelains and glass-ceramics, and 49.0 N for composite IC) and H is hardness ($H = 2P/d^2$, where d is the diagonal of the indentation). After the biaxial flexure tests, the fracture surfaces of all specimens were examined under optical microscopy (DM, RVE, Leica, Wetzlar, Germany) to ensure that fracture occurred from the indentation site.

X-ray diffraction (XRD) analysis (Rigaku, Rint 2000, Tokyo, Japan) was performed on the prepared samples to identify the crystalline phases using Cu Kα radiation at a diffraction angle from 0° to 70°, with a step size of 0.1° and count time per step of 6 s.

Microstructural analyses were performed using a scanning electron microscope (SEM) (JSM 6300, Jeol, Peabody, MA, USA) coupled to an energy dispersive spectroscope (EDS) (Noran Instruments, Middletown, WI, USA). SEM analyses were made after etching with 2% hydrofluoric acid (HF) for 15 s (porcelains and leucite-reinforced glass-ceramic) and 10 min (lithium disilicate glass-ceramic). For In-Ceram

Alumina, no etching was needed to reveal the microstructure [33]. The volume fraction and the size of crystalline particles were determined using an image analyzer software (Leica, QWin, Germany).

Statistical analysis of measured properties data was performed by means of one-way analysis of variance (ANOVA). Tukey's test with a global significance level of 5% was used for multiple comparisons.

3. Results and discussion

The nature of crystalline phases identified by XRD analysis was as follows: tetragonal leucite ($KAlSi_2O_6$) in porcelain D and glass-ceramic E1; mainly lithium disilicate ($Li_2Si_2O_5$) in glass-ceramic E2; and alumina (α-Al_2O_3) in IC composite. Moreover, a broad peak observed in all XRD patterns of these materials indicated the presence of glassy phase. For porcelain V, XRD analysis showed only a broad peak corresponding to the amorphous glass phase and SEM analysis confirmed that this material did not present second-phase particles. The distribution of the leucite particles in the glassy matrix of porcelain D was heterogeneous and they had a dendritic morphology, forming clusters with sizes up to 50 μm (Fig. 1a). The leucite particles in glass-ceramic E1 (Fig. 1b) were more homogeneously distributed compared to porcelain D. The volume fractions of leucite in materials D and E1 were 16 and 29 vol%, respectively, and average leucite particle size was around 1 μm for both materials. Needle-like lithium disilicate particles in glass-ceramic E2 were homogeneously dispersed throughout the glassy matrix (Fig. 1c). The volume fraction of lithium disilicate was 58 vol% and the length and thickness of elongated crystals were ~10 and ~1 μm, respectively. For IC, the alumina particles (65 vol%) were homogeneously dispersed in the final composite (Fig. 1d). These particles presented a wide size distribution (from 1 to 20 μm).

Elastic constants, Vickers hardness, inert strength, and fracture toughness results for the materials tested are shown in Table 2. The Young's modulus and Poisson's ratio values were significantly higher for composite IC, followed by glass-ceramic E2. Glass-ceramic E1 and porcelains V and D presented statistically similar values for both elastic constants. With regards to Vickers hardness, IC showed the highest mean value, followed by glass-ceramic E1 and porcelains V and D, which presented statistically similar values. Glass-ceramic E2 showed the lowest hardness value. The inert strength and fracture toughness values were significantly higher for composite IC and glass-ceramic E2 compared to the other materials. Also, glass-ceramic E1 showed higher mean inert

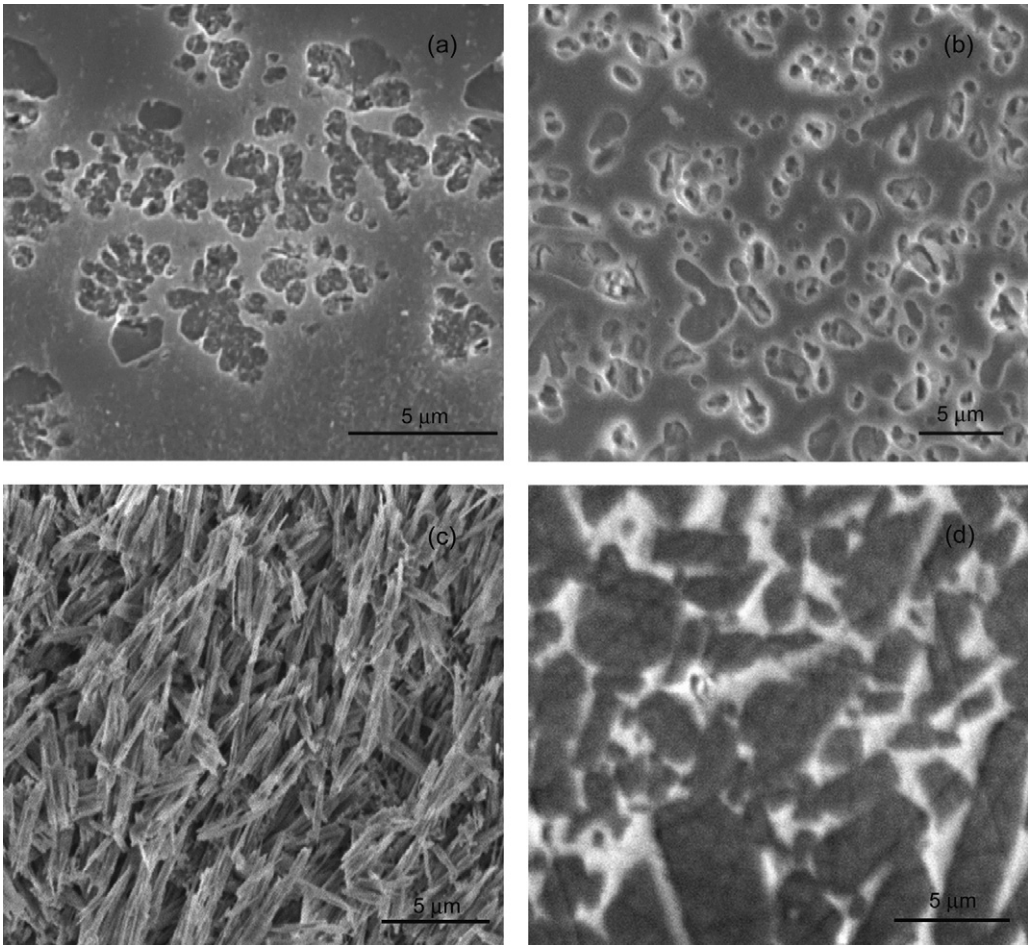

Fig. 1. SEM micrographs of: (a) porcelain D with leucite particles in glassy matrix; (b) glass-ceramic E1 with leucite particles in glassy matrix; (c) glass-ceramic E2 with lithium disilicate elongated particles (glassy matrix removed by deep etching); and (d) composite IC with alumina particles in glassy matrix.

Table 2
Mean ± standard deviations and coefficient of variation (in parenthesis) for Young's modulus (E), Poisson's ratio (υ), Vickers hardness (HV), inert strength (σ_i), fracture toughness (K_{Ic}), fracture surface energy (γ_f) and index of brittleness (B) for the five materials tested. For each property, values followed by the same superscript are statistically similar ($p > 0.05$).

	V	D	E1	E2	IC
E (GPa)	66.0 ± 0.9 (1%)^{c}	67.1 ± 0.6 (1%)^{c}	66.1 ± 1.1 (2%)^{c}	99.3 ± 2.5 (3%)^{b}	276.0 ± 6.5 (2%)^{a}
υ	0.215 ± 0.006 (3%)^{c}	0.217 ± 0.003 (1%)^{c}	0.210 ± 0.007 (3%)^{c}	0.225 ± 0.012 (5%)^{b}	0.239 ± 0.008 (3%)^{a}
HV (GPa)	8.2 ± 0.5 (6%)^{b}	8.0 ± 0.6 (8%)^{b}	7.9 ± 0.4 (5%)^{b}	5.8 ± 0.4 (7%)^{c}	11.2 ± 1.0 (8%)^{a}
σ_i (MPa)	123 ± 22 (17%)^{d}	94 ± 9 (10%)^{d}	167 ± 22 (13%)^{c}	307 ± 38 (12%)^{b}	480 ± 40 (8%)^{a}
K_{Ic} (MPa m$^{1/2}$)	0.67 ± 0.08 (11%)^{d}	0.84 ± 0.07 (8%)^{cd}	0.96 ± 0.03 (4%)^{c}	1.81 ± 0.18 (10%)^{b}	2.91 ± 0.20 (7%)^{a}
γ_f (J/m^2)	3.2	5.0	6.7	15.7	14.5
B (μm$^{-1/2}$)	12.2	9.5	8.2	3.2	3.8

strength and fracture toughness values compared to porcelain D, which showed similar σ_i and K_{Ic} values compared to porcelain V.

The elastic modulus and Vickers hardness values obtained in this study for the five ceramics were in accordance with those reported in the literature [1,2,17,21,22,34–36]. However, a higher hardness value for E2 (lithium disilicate-reinforced glass-ceramic) was expected, since this is a core material for single crowns and small fixed partial dentures up to the premolar region. The lower hardness of E2 may be beneficial if one considers that this value is similar to the hardness of human enamel, 4.9 GPa [37], and therefore when both materials are in contact during mastication, lower wear rates are anticipated in both structures. Since E2 is a core material, direct contact with enamel is not primarily expected, but in posterior regions (premolars and molars) or in prosthesis connectors where greater strength is required one can choose not to use a veneering porcelain over the E2 core [38]. In such cases, the core material is used alone to build the whole restoration, allowing contact between this glass-ceramic and antagonist teeth.

No correlation was observed between Vickers hardness and Young's modulus (Table 2), indicating that the increase in elastic modulus has not led to an increase in the Vickers hardness. However, other studies using a variety of high strength core ceramic materials have shown a significant and positive correlation between dynamic elastic moduli and true hardness (calculated from the slope of the regression line of the length of Knoop indentation versus square root of indentation load) [21]. It can be speculated that differences in hardness tests and the fact that the reported study used only high strength ceramics in contrast to the present one, which used materials with different mechanical properties and microstructures, were responsible for these differences.

As expected from Eq. (1), a positive fracture toughness (K_{Ic}) dependence of fracture strength (σ_i) was observed for the ceramics tested (Fig. 2a), similarly to the trend observed in a previous work [39]. This result confirms the importance of

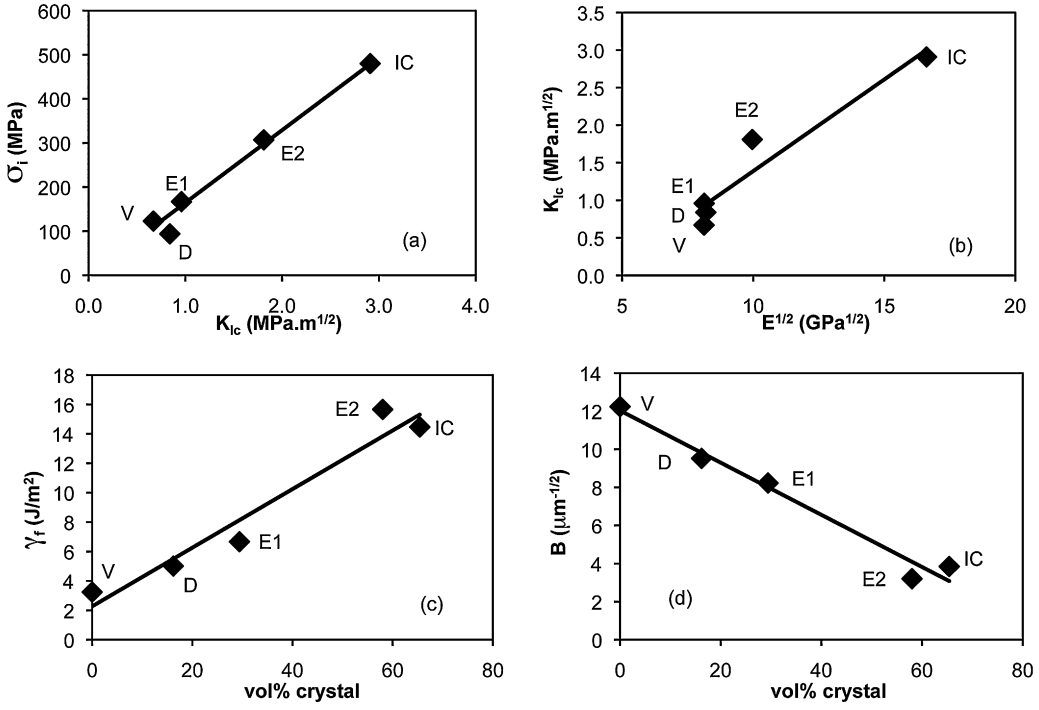

Fig. 2. Correlation plots for the five ceramics tested (V, D-porcelains; E1, E2–glass-ceramics; IC–glass-infiltrated composite): (a) inert strength (σ_i) × fracture toughness (K_{Ic}); (b) K_{Ic} × square root of elastic modulus ($E^{1/2}$); (c) fracture surface energy (γ_f) × crystalline content; and (d) index of brittleness (B) × crystalline content.

enhancing the K_{Ic} value to reduce the brittleness of dental ceramics.

The influence of Young's modulus (E) on the fracture toughness (K_{Ic}) can be theoretically demonstrated, in plane strain, by:

$$K_{Ic} = \sqrt{\frac{2E\gamma_f}{1-\upsilon^2}} \quad (6)$$

where υ is the Poisson's ratio and γ_f is the fracture surface energy, which considers all forms of energy dissipation, including toughening mechanisms [40]. For the data obtained in this work, this theoretical approach was confirmed, since there was a positive correlation between these variables, K_{Ic} and $E^{1/2}$ (Fig. 2b), as predicted by Eq. (6).

Eq. (6) was used to calculate the fracture surface energy (γ_f) for each material using the K_{Ic} and E mean values determined experimentally (Table 2). For this reason, only a mean value of γ_f was determined and no statistical analysis was performed for this parameter. For the two porcelains and the leucite-based glass-ceramic, the γ_f values (between 3.2 and 6.7 J/m^2) were similar to the ones reported in the literature for glasses and glass-ceramics with less than 40% in volume of second phase particles (between 3.3 and 6.4 J/m^2) [41,42]. Materials with higher crystalline content, such as glass-ceramic E2 and composite IC, showed higher fracture surface energy values (15.7 and 14.5 J/m^2, respectively), which were comparable to those obtained in a previous work for polycrystalline alumina (~20 J/m^2) [43]. A positive correlation between γ_f and crystalline content was observed (Fig. 2c). The fracture surface energy of a ceramic material has been defined as the energy absorbed during the extension of a crack over the unit area of surface formed during the fracture process. This parameter controls the fracture process and helps to understand the mechanisms affecting the fracture of solids, being considered a key parameter for the design of ceramic materials [42,44].

Fracture toughness, as shown in Eq. (6), is a function of both elastic modulus (E) and fracture surface energy (γ_f). For porcelains V and D, and glass-ceramic E1, the relatively low fracture toughness values (0.67, 0.84 and 0.96 MPa m$^{1/2}$, respectively) may be related to the low E and γ_f values. Although glass-ceramic E2 showed the highest γ_f value, its relatively low E value resulted in an intermediate K_{Ic} value (1.81 MPa m$^{1/2}$). The alumina-glass composite IC presents a relatively high K_{Ic} value (2.81 MPa m$^{1/2}$) because of its high E and γ_f values (Table 2).

The microstructures of IC and E2 are also responsible for the higher fracture toughness (about three- and two-fold that of porcelains, respectively) compared to other materials tested. For these two ceramics (IC and E2), the higher values of fracture toughness cannot be attributed only to their higher crystalline content. The higher mean particle length (~10 μm for E2 and ~20 μm for IC) and the higher aspect ratio (shape factor) compared to the leucite particles in porcelain D and glass-ceramic E1 (mean particle size of ~1 μm) may also have played an important role in determining this mechanical property, especially because of crack deflection toughening mechanisms. Porcelains V and D and leucite-based glass-ceramic E1 presented relatively straight cracks compared to tortuous crack paths observed in glass-ceramic E2 and glass infiltrated alumina composite IC. It can also be inferred that the crack deflection in ceramics E2 and IC is also responsible for the high fracture surface energy values determined for these materials (15.7 and 14.5 J/m^2, respectively), since the roughness of the fracture surface, characteristic of materials showing such toughening mechanisms, can be correlated to the higher γ_f values. Thus, the results of microstructural characterization (volume fraction of crystals) showed the deflection of cracks as one of the important toughening mechanisms in the materials tested in the present investigation, which have in common the presence of a glassy phase with a volume fraction higher than about 30%.

The index of brittleness (B), which takes into consideration the resistance to deformation and resistance to fracture [25], was calculated using the following equation:

$$B = \frac{HV}{K_{Ic}} \quad (7)$$

where HV is the Vickers hardness. Brittleness increases with the increase in this index. The calculated mean values of B for all tested materials are shown in Table 2. The highest B values were observed for porcelains V and D, and glass-ceramic E1 (12.2, 9.5 and 8.2 μm$^{-1/2}$, respectively) and the lowest for composite IC and glass-ceramic E2 (3.8 and 3.2 μm$^{-1/2}$, respectively). These values were similar to those reported for other ceramics (9 and 3 μm$^{-1/2}$ for silica glass and MgO-doped polycrystalline alumina, respectively) [25]. Poor correlations were observed between B values and E or HV values, but an inverse correlation with the volume fraction of the crystal phase was observed (Fig. 2d). This result suggests that the index of brittleness (B) can be related to the fracture surface energy, γ_f (Fig. 2c).

As mentioned before, the index of brittleness can be more useful for situations involving scratch, wear, erosion and machining of ceramics [24], which can occur during the preparation, marginal fitting, and clinical use of dental restorations [45,46]. These events can introduce surface flaws, a crack initiation process which weakens the restoration. For instance, a scratch created during mastication of a hard food can induce the formation of small surface cracks which will extend subcritically enhanced by the humid oral environment (slow crack growth) up to the critical size. When K_{Ic} is reached, even a low masticatory stress can result in catastrophic failure [47,48]. Therefore, it is important to develop dental ceramics with low index of brittleness (B) which can hinder the crack initiation process.

Based on the fracture mechanics principles outlined in the present study, one can predict and quantify the relationships between mechanical properties, stress level, the presence of crack-producing flaws, and crack propagation mechanisms [18]. In this context, understanding the importance of microstructural characteristics, mechanical properties and fracture behavior is key to the design and development of

new materials for dental applications with improved clinical performance and longevity.

4. Conclusion

Glass-infiltrated alumina composite and lithium disilicate glass-ceramic showed higher values of inert fracture strength (σ_i), Young's modulus (E), fracture toughness (K_{Ic}) and fracture surface energy (γ_f), and lower values of index of brittleness (B) compared to leucite-based glass-ceramic and porcelains. The increase in a material's elastic modulus tends to increase the fracture toughness of dental ceramics, but not necessarily the hardness. The increase of crystalline phase content is beneficial to decrease the brittleness of dental ceramics by means of both increasing the fracture surface energy and decreasing the index of brittleness.

Acknowledgments

The authors acknowledge the Brazilian agencies FAPESP, CNPq and CAPES for the financial support of the present research.

References

[1] M. Albakry, M. Guazzato, M.V. Swain, Fracture toughness and hardness evaluation of three pressable all-ceramic dental materials, J. Dent. 31 (3) (2003) 181–188.
[2] M. Albakry, M. Guazzato, M.V. Swain, Biaxial flexural strength, elastic moduli, and X-ray diffraction characterization of three pressable all-ceramic materials, J. Prosthet. Dent. 89 (4) (2003) 374–380.
[3] J.R. Kelly, I. Nishimura, S.D. Campbell, Ceramics in dentistry: historical roots and current perspectives, J. Prosthet. Dent. 75 (1) (1996) 18–32.
[4] S.O. Koutayas, M. Kern, All-ceramic posts and cores: the state of the art, Quintessence Int. 30 (6) (1999) 383–392.
[5] A.J. Qualtrough, V. Piddock, Ceramics update, J. Dent. 25 (2) (1997) 91–95.
[6] J. Tinschert, D. Zwez, R. Marx, K.J. Anusavice, Structural reliability of alumina-, feldspar-, leucite-, mica- and zirconia-based ceramics, J. Dent. 28 (7) (2000) 529–535.
[7] A. Shenoy, N. Shenoy, Dental ceramics: an update, J. Conserv. Dent. 13 (4) (2011) 195–203.
[8] F. Zarone, S. Russo, R. Sorrentino, From porcelain-fused-to-metal to zirconia: clinical and experimental considerations, Dent. Mater. 27 (1) (2011) 83–96.
[9] J.F. Esquivel-Upshaw, K.J. Anusavice, H. Young, J. Jones, C. Gibbs, Clinical performance of a lithia disilicate-based core ceramic for three-unit posterior FPDs, Int. J. Prosthodont. 17 (4) (2004) 469–475.
[10] J.A. Sorensen, M. Cruz, W.T. Mito, O. Raffeiner, H.R. Meredith, H.P. Foser, A clinical investigation on three-unit fixed partial dentures fabricated with a lithium disilicate glass-ceramic, Pract. Periodontics Aesthet. Dent. 11 (1) (1999) 95–106, quiz 108.
[11] M.J. Suarez, J.F. Lozano, M. Paz Salido, F. Martinez, Three-year clinical evaluation of In-Ceram zirconia posterior FPDs, Int. J. Prosthodont. 17 (1) (2004) 35–38.
[12] P. Vult von Steyern, O. Jonsson, K. Nilner, Five-year evaluation of posterior all-ceramic three-unit (In-Ceram) FPDs, Int. J. Prosthodont. 14 (4) (2001) 379–384.
[13] C.E. Inglis, Stress in a plane due to the presence of cracks and sharp corners, Trans. Inst. Nav. Arch. 55 (1913) 219–241.
[14] A.A. Griffith, The phenomena of rupture and flow in solids, Philos. Trans. R. Soc. 221 (1920) 163–198.
[15] G.R. Irwin, Fracture dynamics, in: Fracture of Metals, vol. 40A, American Society for Metals, Cleveland, 1948, pp. 147–166.
[16] D.J. Green, An Introduction to the Mechanical Properties of Ceramics, University Press, Cambridge, 1998.
[17] N. Suansuwan, M.V. Swain, Determination of elastic properties of metal alloys and dental porcelains, J. Oral Rehabil. 28 (2) (2001) 133–139.
[18] W.D. Callister Jr., Materials Science and Engineering: An Introduction, 5th ed., John Wiley & Sons, Inc., New York, 2000.
[19] R. Morena, P.E. Lockwood, C.W. Fairhurst, Fracture toughness of commercial dental porcelains, Dent. Mater. 2 (2) (1986) 58–62.
[20] D.W. Jones, The strength and strengthening mechanisms of dental ceramics, in: J.L. McLean (Ed.), Dental Ceramics: Proceedings of the First International Symposium on Ceramics, 1983.
[21] A.S. Rizkalla, D.W. Jones, Mechanical properties of commercial high strength ceramic core materials, Dent. Mater. 20 (2) (2004) 207–212.
[22] A.S. Rizkalla, D.W. Jones, Indentation fracture toughness and dynamic elastic moduli for commercial feldspathic dental porcelain materials, Dent. Mater. 20 (2) (2004) 198–206.
[23] G.D. Quinn, Fractography of Ceramics and Glasses, National Institute of Standards and Technology, Washington, 2007.
[24] J.B. Quinn, G.D. Quinn, Indentation brittleness of ceramics: a fresh approach, J. Mater. Sci. 32 (16) (1997) 4331–4346.
[25] B.R. Lawn, D.B. Marshall, Hardness, toughness, and brittleness: an indentation analysis, J. Am. Ceram. Soc. 62 (7–8) (1979) 347–350.
[26] ASTM-C1161, Standard Test Method for Flexural Strength for Advanced Ceramics at Ambient Temperature, American Society for Testing Materials, West Conshohocken, 2002.
[27] ASTM-E-494-95, Standard Practice for Measuring Ultrasonic Velocity in Materials, American Society for Testing Materials, West Conshohocken, 2001.
[28] H.N. Yoshimura, A.L. Molisani, N.E. Narita, P.F. Cesar, H. Goldenstein, Porosity dependence of elastic constants in aluminum nitride ceramics, Mater. Res. 10 (2) (2007) 127–133.
[29] ASTM-F394-78, Standard Test Method for Biaxial Flexure Strength (Modulus of Rupture) of Ceramic Substrates, American Society for Testing Materials, West Conshohocken, 1996.
[30] C.C. Gonzaga, P.F. Cesar, W.G. Miranda, H.N. Yoshimura Jr., Slow crack growth and reliability of dental ceramics, Dent. Mater. 27 (4) (2011) 394–406.
[31] ASTM-C1327, Standard Test Method for Vickers Indentation Hardness of Advanced Ceramics, American Association for Testing Materials, West Conshohocken, 1999.
[32] P. Chantikul, G.R. Anstis, B.R. Lawn, D.B. Marshall, A critical evaluation of indentation techniques for measuring fracture toughness: II, strength method, J. Am. Ceram. Soc. 64 (9) (1981) 539–543.
[33] C.C. Gonzaga, H.N. Yoshimura, P.F. Cesar, W.G. Miranda Jr., Subcritical crack growth in porcelains, glass-ceramics, and glass-infiltrated alumina composite for dental restorations, J. Mater. Sci. Mater. Med. 20 (5) (2009) 1017–1024.
[34] M. Guazzato, M. Albakry, S.P. Ringer, M.V. Swain, Strength, fracture toughness and microstructure of a selection of all-ceramic materials. Part I. Pressable and alumina glass-infiltrated ceramics, Dent. Mater. 20 (5) (2004) 441–448.
[35] R.R. Seghi, I.L. Denry, S.F. Rosenstiel, Relative fracture toughness and hardness of new dental ceramics, J. Prosthet. Dent. 74 (2) (1995) 145–150.
[36] G. Sinmazisik, M.L. Ovecoglu, Physical properties and microstructural characterization of dental porcelains mixed with distilled water and modeling liquid, Dent. Mater. 22 (8) (2006) 735–745.
[37] E. Mahoney, A. Holt, M. Swain, N. Kilpatrick, The hardness and modulus of elasticity of primary molar teeth: an ultra-micro-indentation study, J. Dent. 28 (8) (2000) 589–594.
[38] J.F. Esquivel-Upshaw, H. Young, J. Jones, M. Yang, K.J. Anusavice, In vivo wear of enamel by a lithia disilicate-based core ceramic used for posterior fixed partial dentures: first-year results, Int. J. Prosthodont. 19 (4) (2006) 391–396.
[39] P.F. Cesar, H.N. Yoshimura, W.G. Miranda, C.L. Miyazaki Jr., L.M. Muta, L.E. Rodrigues Filho, Relationship between fracture toughness and flexural strength in dental porcelains, J. Biomed. Mater. Res. B Appl. Biomater. 78 (2) (2006) 265–273.

[40] J.B. Wachtman, Mechanical Properties of Ceramics, John Wiley & Sons, New York, 1996.
[41] T. Kokubo, S. Ito, M. Shigematsu, T. Yamamuro, Mechanical properties of a new type of apatite-containing glass-ceramic for prosthetic application, J. Mater. Sci. 20 (1985) 2001–2004.
[42] S.M. Wiederhorn, Fracture surface energy of glass, J. Am. Ceram. Soc. 52 (2) (1969) 99–105.
[43] R.W. Rice, S.W. Freiman, P.F. Becher, Grain size dependence of fracture energy in ceramics: I, experimental, J. Am. Ceram. Soc. 64 (6) (1981) 345–349.
[44] J.A. Coppola, R.C. Bradt, Measurement of fracture surface energy of SiC, J. Am. Ceram. Soc. 55 (9) (1972) 455–460.
[45] R.M.C. Sasahara, F.C. Ribeiro, P.F. Cesar, H.N. Yoshimura, Influence of the finishing technique on surface roughness of dental porcelains with different microstructures, Oper. Dent. 31 (5) (2006) 577–583.
[46] H.N. Yoshimura, P.F. Cesar, F.N. Soki, C.C. Gonzaga, Stress intensity factor threshold in dental porcelains, J. Mater. Sci. Mater. Med. 19 (5) (2008) 1945–1951.
[47] P.F. Cesar, F.N. Soki, H.N. Yoshimura, C.C. Gonzaga, V. Styopkin, Influence of leucite content on slow crack growth of dental porcelains, Dent. Mater. 24 (8) (2008) 1114–1122.
[48] M.M. Pinto, P.F. Cesar, V. Rosa, H.N. Yoshimura, Influence of pH on slow crack growth of dental porcelains, Dent. Mater. 24 (6) (2008) 814–823.